ELSEVIER

Polymer 40 (1999) 2331–2346

polymer

Toughness mechanism in semi-crystalline polymer blends: I. High-density polyethylene toughened with rubbers

Z. Bartczak[1a], A.S. Argon[a,*], R.E. Cohen[a], M. Weinberg[b]

[a]*Massachusetts Institute of Technology, Cambridge, MA 02139, USA*
[b]*E.I. du Pont de Nemours & Co., Central Research and Development, Experimental Station, Wilmington, DE 19898, USA*

Received 12 December 1997; revised 1 May 1998; accepted 2 June 1998

Abstract

The mechanical response of rubber-modified high density polyethylene (HDPE) was investigated. The rubbers were either ethylene–propylene copolymers (EPDM) or ethylene–octene copolymers (EOR), blended into HDPE at volume fractions of up to 0.22. These rubbers were in the form of finely dispersed spherical inclusions with sizes well below 1 μm. The incorporation of rubber into HDPE does not substantially change its crystallinity, but produces special forms of preferential crystallization around the rubber particles. The notch toughness of the rubber-modified HDPE increases by more than 16-fold as a result. The single parameter, controlling the notch toughness of these blends was found to be the matrix ligament thickness between rubber inclusions. When this thickness is above a certain critical value, the notch toughness of the material remains as low as that of the unmodified HDPE. When the average ligament thickness is less than the critical value a dramatic toughness jump results. The critical ligament thickness for the HDPE–rubber systems was found to be around 0.6 μm, independent of the type of the rubber used. The sharp toughness threshold in the rubber-modified HDPEs results from a specific micro-morphology of the crystalline component of HDPE surrounding the rubber particles. The PE crystallites of approximately 0.3 μm length perpendicular to the interface are primarily oriented with their (100) planes parallel to the particle interfaces. Material of this constitution has an anisotropic plastic resistance of only about half that of randomly oriented crystallites. Thus, when the interparticle ligaments of PE are less than 0.6 μm in thickness the specially oriented crystalline layers overlap, and percolate through the blend, resulting in overall plastic resistance levels well under that which results in notch brittle behaviour, once rubbery particles cavitate in response to the deformation-induced internal negative pressure. This renders ineffective the usual strength-limiting microstructural flaws and results in superior toughness at impact strain rates.

Keywords: Toughness; Semi-crystalline polymer; Polyethylene

1. Introduction

Many semi-crystalline engineering polymers including Nylon, isotactic polypropylene and linear polyethylene exhibit very attractive strength and ductility at room temperature and under moderate rates of deformation. However, they become brittle under severe conditions of deformation such as low temperature or high strain rates, and can undergo a sharp ductile-to-brittle transition. In the brittle regime a crack can propagate with little resistance. Because of this poor performance at extreme conditions there has been considerable commercial and scientific interest in the toughening of semi-crystalline engineering thermoplastics [1,2].

The brittle–ductile transition can be attributed to a competition between brittle behaviour characterized by a brittle strength, governed by microstructural flaws, and energy-absorbing plastic response, both having different temperature and strain rate dependence (Ludwik–Davidenkow–Orowan model; see, e.g. Ref. [3]). While the brittle strength, σ_B, of the material can be considered to be nearly temperature independent and flaw-governed, the plastic resistance, Y, characterizing the ductile response has substantial temperature and strain rate dependence. Therefore, for a given strain rate a ductile to brittle transition can be expected to occur at a temperature where Y rises above σ_B. This transition temperature increases with increasing strain rate due to the sensitivity of Y on strain rate. Moreover, while σ_B relates to a tensile response, the plastic behaviour responds only to a critical level of the effective (deviatoric) stress, σ_e. In the presence of sharp notches or cracks, individual stress components can be substantially augmented by a negative

* Corresponding author.
[1] Permanent address: Centre of Molecular and Macromolecular Studies, Polish Academy of Sciences, 90-363 Lodz, Poland.

0032-3861/99/$ - see front matter
PII: S0032-3861(98)00445-5

pressure present in the notch field, while the effective stress producing plastic flow remains equal to *Y*. This, plus the elevation of *Y* itself due to severe strain rate concentration around notches will lead to marked increases in the brittle–ductile transition temperature. Consequently, when structural imperfections, such as notches, crack-like flaws or poorly adhering large foreign particles, are present in the material in the size range of about 10 μm, they will result in a brittle response of the material. However, if the structural imperfections are well controlled and foreign particles are only in the sub-micron range, the brittle strength of polymers can be increased somewhat to suppress the ductile-to-brittle transition to lower temperatures. Thus, when the yield strength falls below the brittle strength and plastic response is initiated, it often results in neutralization of the effect of some of the imperfections by molecular alignment or texture development that can significantly elevate the fracture stress across the principal direction of extension.

The above elementary outlined considerations of the brittle–ductile transition lead to the conclusion that, apart from chemical modification which changes the intrinsic properties of a polymer [1], there are two basic routes of increasing toughness of polymeric materials: either by reinforcing them (e.g. with long, high-strength fibres) in order to increase their brittle strength, or by incorporation of fine particles, which directly or indirectly reduce the overall plastic resistance of the material. Both methods are frequently used in engineering practice. In spite of numerous experimental and theoretical studies, however, the mechanistic understanding of such practices in the successful modification of polymer behaviour, but especially in the field of rubber-toughening of semi-crystalline polymers, has remained unsatisfactory.

The toughening of the semi-crystalline polymers with rubber particles has been extensively studied over the last two decades. Most of these studies have concentrated on polyamides (e.g. Refs. [4–13]) and isotactic polypropylene (see, e.g. Refs. [2,14]), because of the special practical importance of these materials. It is beyond the scope of this communication to provide a review of the abundant literature on this topic. We note, however, several studies that have documented the effect of parameters such as rubber particle size [6,11], volume fraction and inter-particle distance [4,5] on the effectiveness of toughening by this practice. The general conclusion drawn in these studies was that for a blend to be tough, the particles must be smaller than a critical size which depends on the matrix type and rubber concentration. Similarly, the rubber concentration must be above a critical level which, in turn, is a function of particle size. Clearly, these conclusions lack precision.

The most important conclusion in these earlier studies, based on experimental observations, was reached by Wu [4,5], who demonstrated that the key parameter for rubber toughening is the thickness of the matrix ligaments between rubber particles. This single parameter was directly related to both rubber concentration and average size of particles. Wu demonstrated this effect by using a series of rubber-modified polyamide-6,6 blends, that regardless of particle size and rubber concentration were tough if the matrix ligament thickness was kept below a critical value, which for polyamide-6,6 was 0.3 μm. Explanations offered by Wu [4,5], however, to account for this finding, based on arguments of field theory, were unacceptable, since field theory is scale independent.

Recently Muratoglu et al. [12] proposed a new morphological explanation of Wu's observations based on the critical ligament dimension. They observed by TEM that, in Nylon 6,6 modified with EPR rubber, when the interparticle ligaments are less than a critical dimension the Nylon matrix within the ligaments has a specific crystallographic orientation, with the crystalline lamellae being arranged perpendicular to the interfaces of adjacent rubber particles with the matrix [12]. In a detailed model study of thin films of Nylon 6 melt-crystallized between two thin sheets of EPR rubber they found [15] that in this preferential orientation of lamellae the low energy hydrogen-bonded crystallographic (001) planes were parallel to the interfaces of the rubber substrates with, however, the chain orientation being random within this plane. Such oriented layers of lamellae extended approximately 0.15 μm away from each rubber-Nylon interface, and in films of thickness less than 0.3 μm produced preferred orientation throughout the film. However, when the film thickness exceeded 0.3 μm crystallites of random orientation were found to populate the interior. TEM observations showed that an analogous situation arose in the rubber-modified blend, where strong crystallographic orientation develops between rubber particles, when ligaments were thinner than 0.3 μm. The plastic shear resistance for chain slip in (001) planes of Nylon 6 is known to be only half of that of any other crystallographic slip system and, hence, lower than the overall polycrystal average plastic resistance of material with randomly oriented crystallites [16]. Thus, upon inception of deformation after rubber particles cavitate, the resulting cellular material will have a substantially lowered plastic resistance when the thickness of the interparticle ligaments in the blend is less than 0.3 μm. The reduced overall plastic resistance then, prevents premature fracture emanating from pre-existing flaws, and the material exhibits high toughness. Such transition from brittle to tough behaviour with decreasing matrix ligament thickness was in fact observed experimentally by a number of other investigators of rubber-toughened Nylons and polypropylene [4,5,11,17], albeit without a proper explanation.

The mechanism of toughening based on a preferred crystallographic texture in the rubber-modified blend [12], although very attractive, has been demonstrated experimentally only for rubber-toughening of Nylon. The presence of hydrogen bonded planes in Nylon can help produce the specific orientation of crystalline component within matrix ligaments. Therefore, the question arises whether this mechanism is specific for toughening of only Nylons or is

it more general and applicable to the toughening of other notch brittle semi-crystalline polymers?

The goal of this communication is to provide a generalization of the hypothesis of micro-orientation-governed toughness, using a particle-toughened polymer system which does not contain hydrogen bonds in its structure. As a model matrix, a linear high-density polyethylene was chosen, partly because of the extensive information available on its crystallographic mechanisms of deformation [18,19]. For many common applications polyethylene (HDPE) is a tough polymer and does not need further toughening. However, there are numerous special applications under extreme conditions of strain rate and/or temperature for which its toughness needs to be substantially increased. Although there are commercially available methods of increasing the toughness of polyethylene by relatively simple alterations of its chemical structure [17], the method of toughening of the most common HDPE by blending it with rubbers is also widely practiced (Allied Signal has developed a polyethylene-elastomer Paxon Pax® Plus, designed for film applications). Thus, the morphology and mechanical properties, including impact properties, of polyethylene–rubber blends (mostly with EPDM as a rubber component) have been studied by a number of investigators [20–25]. A further very attractive prospect emerging from the mechanism proposed by Muratoglu et al. is that the toughness of the matrix could in principle be greatly improved not only by rubber particles but also by stiff particles such as mineral fillers, provided such filler particles have the appropriate incoherent interfaces to promote oriented crystallization based only on free energy considerations, have the appropriate size and spacing required to satisfy a critical ligament thickness condition, and undergo ready debonding during straining to permit the plastic stretching of the matrix ligaments. Since toughness in this model is the result of lowered plastic resistance afforded by the specific micro-orientation of the matrix, the primary role of particles becomes merely the promotion of oriented crystallization. The investigation of toughening of HDPE using rigid filler particles is described in the companion communication which follows the present one [26].

2. Experimental details

2.1. Materials and sample preparation

The polymers used in this study are listed in the Table 1. Among the rubbers used for HDPE modification three classes can be distinguished: amorphous ethylene–propylene–diene terpolymers (EPDM; codes T1–T3 in Table 1), semi-crystalline EPDMs (codes T4–T7) and semi-crystalline ethylene–octene rubbers (EOR; codes R1–R4). The blends of HDPE with various grades of EPDM and EOR rubbers were prepared by melt-mixing in a 28 mm Werner and Pfleider twin-screw extruder. The extrusion process was performed in the 190–200°C temperature range. The rotation speed of the screws was 200 RPM. Table 2a,b lists the compositions of the prepared blends along with their codes, used throughout this communication.

The extrudates were pelletized and the resulting pellets of the blends were moulded in a 6 oz, 150 ton Van Dorn injection-moulding machine into dog-bone-shaped tensile bars (ASTM D638-95 Type I specimen, 50 mm gauge length,

Table 1
Characteristics of polymers used in the present study

Code	Polymer	Trade name	Supplier	Typical M_w (g/mol)	M_w distribution	Density (g/cm^3)	MFI (g/10 min)	Mooney viscosity	Crystalline character
PE	High-density polyethylene (HDPE)	Dowlex IP-10	Dow plastics			0.962	9.0		Highly crystalline
T1	Ethylene–propylene–diene terpolymer (EPDM)	Nordel 1070	DuPont Dow Elastomers	210 000	Broad	0.860		68[a]	Amorphous
T2		Nordel 1145		290 000	Narrow	0.870		43[a]	Amorphous (trace of crystallinity)
T3		Nordel 1320		130 000	Narrow	0.870		21[a]	Amorphous
T4		Nordel 2470		230 000	Narrow	0.880		68[b]	Semi-crystalline
T5		Nordel 2760		220 000	Narrow	0.880		60[b]	Semi-crystalline
T6		Nordel 2744		230 000	Narrow	0.880		47[c]	Semi-crystalline
T7		Nordel 2722		180 000	Narrow	0.880		27[a]	Semi-crystalline
R1	Ethylene–octene rubber (EOR)	Engage 8100	DuPont Dow Elastomers	146 000		0.870	1.0	23[c]	Semi-crystalline
R2		Engage 8150		162 700		0.868	0.5	35[c]	Semi-crystalline
R3		Engage 8200				0.870	5.0	8[c]	Semi-crystalline
R4		Engage 8400				0.870	30.0	1.5[c]	Semi-crystalline

[a] ML 1 + 4 at 125°C
[b] ML 2 + 10 at 125°C
[c] ML 1 + 4 at 121°C

Table 2
Composition of the prepared blends and their tensile properties

Blend code	Rubber name	Volumetric composition (PE/R)	Young's modulus (MPa)	Stress at yield[a] (MPa)	Stress at break[a] (MPa)	Ultimate elongation (%)	Natural draw ratio
(*a*) Constant rubber fraction, $\phi = 0.22$							
PE (control)		100:0	756.1	24.85	17.5	730	9
PE-T1–22	Nordel 1070	78:22	356.6	13.50	14.8	620	5
PE-T2–22	Nordel 1145	78:22	304.8	12.84	> 13	> 800	5
PE-T3–22	Nordel 1320	78:22	356.6	13.42	> 11.5	> 800	5
PE-T4–22	Nordel 2470	78:22	285.3	13.20	> 16	> 800	5
PE-T5–22	Nordel 2760	78:22	335.8	14.2	> 17	> 800	5
PE-T6–22	Nordel 2744	78:22	351.0	14.1	> 16	> 800	5
PE-T7–22	Nordel 2722	78:22	329.3	14.25	> 15	> 800	5
PE-R1–22	Engage 8100	78:22	391.2	15.36	17.1	650	5
PE-R2–22	Engage 8150	78:22	385.8	15.51	16.73	640	5.5
PE-R3–22	Engage 8200	78:22	384.6	15.40	> 16	> 800	6.5
PE-R4–22	Engage 8400	78:22	381.4	15.33	> 16	> 800	7
(*b*) Blends with various rubber content							
PE-T1–05	Nordel 1070	95:5	598.4	21.16	16.0	730	8
PE-T1–10	Nordel 1070	90:10	474.9	18.59	> 16	> 750	7.5
PE-T1–15	Nordel 1070	85:15	361.3	16.28	15.6	690	6.5
PE-T1–20	Nordel 1070	80:20	319.4	14.34	13.9	635	6
PE-T1–22	Nordel 1070	78:22	356.6	13.50	14.8	620	5
PE-T7–05	Nordel 2722	95:5	611.7	22.46	14.5	770	8
PE-T7–10	Nordel 2722	90:10	522.6	20.36	15.0	795	8
PE-T7–15	Nordel 2722	85:15	427.0	18.50	13.5	760	7.5
PE-T7–20	Nordel 2722	80:20	382.7	17.24	> 13.5	> 800	6.5
PE-T7–22	Nordel 2722	78:22	329.3	14.25	> 14.5	> 800	5
PE-R1–05	Engage 8100	95:5	629.9	21.87	16.2	620	8
PE-R1–10	Engage 8100	90:10	530.9	19.90	> 17.8	> 800	7.5
PE-R1–15	Engage 8100	85:15	469.3	18.02	> 18	> 800	6.5
PE-R1–20	Engage 8100	80:20	419.5	16.61	17.3	650	5.5
PE-R1–22	Engage 8100	78:22	391.2	15.36	17.1	650	5
PE-R4–05	Engage 8400	95:5	620.2	21.69	17.2	730	8
PE-R4–10	Engage 8400	90:10	507.2	19.74	14.3	760	7.5
PE-R4–15	Engage 8400	85:15	458.4	17.89	14.5	790	7.5
PE-R4–20	Engage 8400	80:20	393.6	16.23	> 14	> 800	7.2
PE-R4–22	Engage 8400	78:22	381.4	15.33	> 13	> 800	7

[a]Engineering stress related to initial sample cross-section

12.7 mm width, and 3.2 mm thickness) and flexural test bars (127 mm length, 12.7 mm width, and 3.2 mm thickness). Temperature of the barrel was 190°C while the mould was kept at 60°C. The injection-moulded flexural bars were then divided into two 63.5 mm long pieces, one close to the gate (called hereafter the *gate end*) and the other far from the gate (called hereafter the *far end*). Notches of root radius 0.254 mm were cut into each part with a TMI Notching Cutter according to the specifications of ASTM D-256.

2.2. Mechanical properties

The tensile properties of the dog-bone-shaped specimens of the blends were studied at room temperature using an Instron 4201 tensile testing machine. The tests were performed according to ASTM D638-95 specification at 50 mm/min crosshead speed, resulting in an initial strain rate of $1.67 \times 10^{-2}\ s^{-1}$.

The impact response was studied in notched Izod impact tests performed according to ASTM D-256 standards. The pendulum speed at impact was 3.45 m/s. The tests were conducted at temperatures ranging from −70°C up to room temperature. Kinetic and frictional energy corrections were made in all tests in accordance with ASTM D-256 standards. Because of the possible influence of the conditions of the injection moulding process specimens obtained from the *gate end* and *far end* of the flexural bars were tested in separate series.

The samples were not conditioned prior to testing to remove water because in polyolefins the influence of water on mechanical properties is negligible. Nevertheless, all specimens were handled according to exactly the same procedures prior to testing: i.e. immediately after injection moulding and/or cutting notches, the specimens were sealed in air-tight bags under a dry nitrogen blanket and were kept in a dessicator until they were tested.

The values of the mechanical parameters determined from both tensile and Izod tests were calculated as averages over measurements on at least five specimens for each composition and test condition.

2.3. Scanning electron microscopy

For SEM observations an Environmental Scanning Microscope, E-SEM (ElectroScan), equipped with LaB_6 filament, was used. This microscope operates under adjustable water vapour pressure in the range of 0.1–10 Torr. This moist environment in the specimen chamber helps preventing electron charging on insulating surfaces. Although charging of the samples was not an issue, a thin (20 nm) coating of gold/palladium was applied to improve image resolution. The accelerating voltage of the microscope was usually set to be in the range of 10–15 kV.

To estimate the particle size in the selected blends the undeformed rubber-modified HDPE, tension specimens were first sectioned perpendicular to the flow direction in the mould and subsequently the undamaged surfaces were exposed by means of microtoming with a freshly prepared glass knife, followed by etching with hot xylene vapours for 2 s. The etching time was short enough to avoid excessive attach of the HDPE matrix while being sufficiently long to dissolve the rubber inclusions. The size of the rubber inclusions was then determined by image analysis of the SEM micrographs of etched surfaces of the blends (Image-Pro® Plus by Media Cybernetics, MD).

The E-SEM was also used to study the morphology of fracture surfaces of the Izod samples as well as the cavitation in the bulk of these deformed samples. The latter was accomplished by cryofracturing the broken Izod samples along two different planes, IZOD1 and IZOD2, shown schematically in Fig. 1. The cryofracturing along IZOD1 and IZOD2 planes exposed the bulk morphology of the cavitated blend and the internal structure of the cavities in the intensely deformed regions near the crack flanks in planes parallel and perpendicular to the crack tip, respectively. The cryofracture was performed by introducing notches along the desired directions followed by soaking in liquid nitrogen for 20 min. A wedge was then driven into the notches to cleave the specimen along the desired planes while it was still at liquid nitrogen temperature. The exposed internal surfaces were then coated with gold/palladium and examined under the E-SEM.

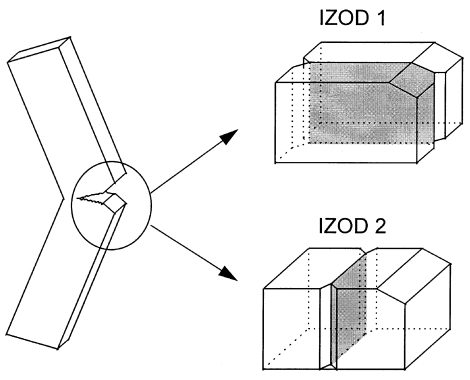

Fig. 1. Modes of cryofracturing of the Izod samples for E-SEM.

2.4. Thermal analysis

The melting and crystallization behaviour of the rubber-modified HDPE was studied by differential scanning calorimetry (DSC 7, Perkin-Elmer) at cooling and heating rates of 10 K/min. Prior to a crystallization run, all specimens were melted at 200°C and kept at this temperature for 5 min. For determination of crystallinity of the HDPE component of the blends a value of 293 J/g was used as the heat of fusion of 100% crystalline polyethylene [27].

3. Results

3.1. Morphology

SEM observations demonstrated that all the blends investigated exhibit distinct phase separation of components. In these HDPE constitutes a topologically continuous matrix in which the rubber inclusions are dispersed. This observation agrees with the previous studies of morphology of HDPE/rubber blends [21–25]. The diameter of the rubber inclusions depends on the particular type of the rubber, but generally does not exceed 1μm. The quantitative estimation of the sizes of the rubber inclusions was done using image analysis of SEM micrographs for two pairs of blends: HDPE with EPDM (PE-T1–22 and PE-T7–22) and HDPE with EOR (PE-R1–22 and PE-R4–22). The T1 and T7 EPDM blends had extreme viscosities in their class, as did the R1 and R4 blends containing EOR.

The distributions of rubber particle size in these blends were close to a simple log-normal distribution but were slightly truncated on the side of the smallest particle sizes, possibly due to sampling errors in such microscopy, which frequently underestimates fractions of the smallest particles. The relevant parameters of particle size distributions are reported in Table 3. Average sizes of rubber inclusion in other blends are likely to fall within these limits, as properties of the rubbers in them are intermediate between those of R1 and R7 or T1 and T4.

In order to study the influence of the rubber type on the formation of the crystalline component of the HDPE matrix, d.s.c. studies of non-isothermal crystallization and melting behaviour were carried out. Both cooling (crystallization) and heating (melting) scans were run at a rate of 10°C/min. The peak onset and maximum values were determined along with the heat of fusion, from which the crystallinity of the HDPE present in the blend was calculated. To ensure comparable thermal histories for all blends, the samples were melt-annealed for 5 min at 200°C prior to crystallization, as discussed in Section 2.4 above, to destroy self-seeding nuclei and erase any thermal memory. Melting behaviour was studied in the same specimens, after completion of their non-isothermal crystallization and cooling down to 30°C. Fig. 2a presents data obtained for crystallization temperature, while Fig. 2b shows melting temperature, and Fig. 2c

Table 3
Parameters of the distributions of the size of rubber particles for the HDPE–rubber blends

Blend code	Geometrical mean diameter[a] $\langle D_{gn}\rangle$ (μm)	Geometrical standard deviation, σ_g^b	Arithmetical mean diameter[a], $\langle D_{an}\rangle$ (μm)	Arithmetical standard deviation, σ_a (μm)
PE-T1–22	0.504	1.36	0.529	0.152
PE-T7–22	0.870	1.45	0.922	0.260
PE-R1–22	0.366	1.47	0.401	0.150
PE-R4–22	0.694	1.49	0.762	0.282

[a]Geometric mean defined as $\langle D_{gn}\rangle = (\prod_{i=1} nD_i)^{1/m}$ as opposed to arithmetical mean, $\langle D_{an}\rangle = (\sum_{i=1}^{n} D_i)/(\Sigma n_i)$
[b]$\log \sigma = [\sum_{i=1}^{n}(\log D_i - \log\langle D_{gn}\rangle 2/(\sum_{i=1}^{n} n_i)]^{1/2}$; σ has a minimum value of 1 when distribution is monodisperse

the calculated degree of crystallinity. All blends presented here had the same 0.22 vol. fraction of rubber. Incorporation of the rubber into HDPE generally induces a slight decrease of crystallization temperature compared to crystallization of plain HDPE (with the exception of the amorphous EPDMs, T1 and T3, which induce a slight increase). The presence of the rubber in the blends also decreases the temperature of the melting peak of HDPE as well as its crystallinity. These data demonstrate that neither the rubbers incorporated into HDPE nor their additives (stabilizers, etc.) had any significant influence on the nucleation of crystallites in PE. The observed changes in the crystallization and melting behaviour of HDPE in the blends, although not dramatic, can improve to some extent the impact properties of the HDPE matrix as compared to plain HDPE. When PE crystallizes at lower temperatures, as in the case of the blends investigated here, the crystallites are thinner, indicated by a slightly lower melting temperature in blends. Moreover, due to faster growth at lower crystallization temperatures, the crystallites are expected to be less perfect and connected by larger concentrations of tie molecules. These features by themselves are known to improve the impact resistance of polyethylene to some extent [18]. However, as we will demonstrate below, these effects are not of major importance in achieving high toughness of the rubber-modified HDPE, but could make some contributions to the overall performance of these systems that must be recognized.

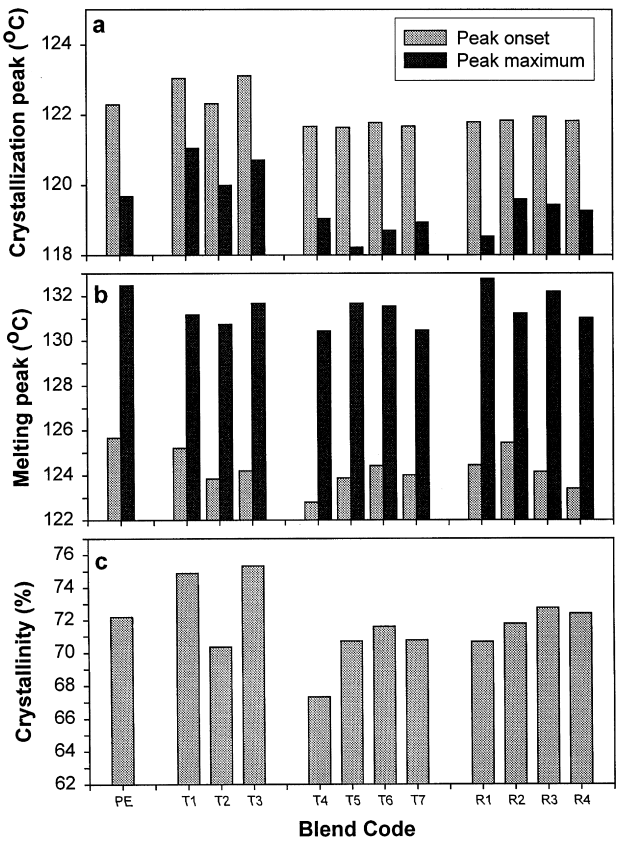

Fig. 2. D.s.c. data for temperatures of nonisothermal (a) crystallization peaks, (b) melting peaks, and (c) the crystallinity of HDPE determined from the melting scan. Light grey bars show the onset while dark grey bars give the temperature at peak level. All blends shown have the same volumetric composition (78:22). The codes T1 through R4 denote the rubber type according to Table 1, while PE means the reference sample of plain HDPE.

3.2. Tensile properties

Table 2a shows the results of tensile tests on the series of HDPE modified with EPDM and EOR rubbers. As before, all blends presented in this table have the same volume fraction of 0.22 of rubber and were processed at identical conditions. The elastic moduli as well as yield and fracture parameters were determined from the stress–strain curves. We note, however, that the reported values of ultimate elongation of the blends are merely estimates, since in the advanced stages of their plastic deformation the necked zone of specimens frequently extended beyond the narrow gauge sections, which made determinations based on overall machine displacement inaccurate. For these samples the reported elongations are lower limits.

The specimens were imprinted with ink markers prior to the test. This allowed the estimation of the natural draw ratio of the blends by measuring the distance between the markers within the necked portion of the deforming specimens (this measurement was always performed before the neck extended over the whole gauge section of the specimen and strain hardening set in). The estimated natural draw ratios are reported in the last column of Table 2a.

Analogous mechanical data obtained from the tensile tests of the blends of HDPE with four selected EPDM and EOR rubbers are presented in Table 2b. Here the volume

fraction of rubber incorporated into HDPE varied from 0 to 0.22. These data show that the tensile properties change gradually with increasing rubber fraction in the blend and there is no abrupt transition of any mechanical parameter in the composition range studied.

The data presented in Table 2a demonstrate that the incorporation of a volume fraction of 0.22 of a rubber into HDPE matrix causes a decrease in the Young's modulus, *E*, by 50%–60% and yield stress, *Y*, by 40%–50%, relative to the unmodified HDPE. In contrast, the ultimate elongation of the blends is usually higher, while the stress at break is in the same range or slightly lower than that of HDPE. The moduli and yield stresses observed for HDPE/EOR blends are somewhat higher than those for HDPE/EPDM blends. An additional difference between HDPE/EPDM and HDPE/EOR blends is in the appearance of the blends during the deformation process. While HDPE and HDPE/EOR blends undergo some whitening in the necked zone, the HDPE/EPDM blends become transparent at the same stage of deformation. They start to whiten later in the deformation process, when strain hardening occurs and the stress rises. Even so, the HDPE/EPDM samples remain relatively transparent compared to other blends or unmodified HDPE. Whitening of the material during its tensile deformation is generally a manifestation of a fine-scale cavitation process. This suggests that the EPDM inclusions neither cavitate nor debond from the HDPE matrix during the plastic flow under conditions used in the reported tensile tests. Still attached to the plastically deforming HDPE matrix, they undergo high extension. Because of good adhesion between rubber and HDPE the highly extended inclusions constrain further plastic deformation of the HDPE matrix, which in turn prevents the cavitation of the matrix itself. Higher stress, as in the strain-hardening region, and/or higher deformation rate is necessary to induce the cavitation or debonding of these EPDM rubber inclusions. It will be demonstrated later in this section that extensive cavitation occurs for both EPDM and EOR rubbers in the high-speed impact tests where the plastic resistances reach significantly higher levels. The influence of non-cavitating and non-debonding EPDM particles on the development of plastic deformation of the matrix can be confirmed by comparison of the natural draw ratios of HDPE/EPDM blends with those of HDPE and HDPE/EOR blends. This ratio for HDPE is close to 9, while it is reduced to only 5 for HDPE/EPDM blends. In the HDPE/EOR blends which seem to undergo cavitation during plastic flow, the natural draw ratio varies from 5 to 7. The values observed for HDPE/EOR blends suggest that in these blends too the cavitation of the rubber is limited. In fact, although these blends whiten during plastic deformation, the whitening is not as strong as in unmodified HDPE.

In spite of the differences outlined above in the tensile deformation behaviour of the blends containing various rubbers, the differences in the mechanical properties observed among these blends are much smaller than those between rubber-modified and plain HDPE, demonstrating that the choice of the particular rubber is of minor importance, at least from the point of view of tensile properties.

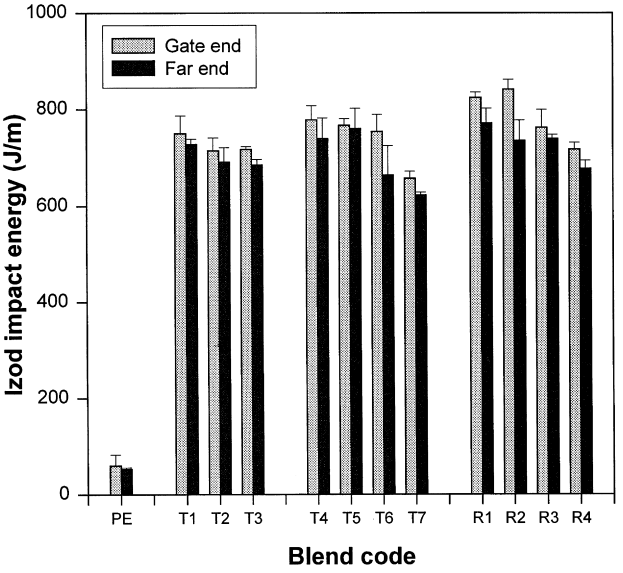

Fig. 3. The dependence of the notched Izod impact energy of HDPE–rubber blends on the type of rubber. All blends shown have the same volumetric composition (78:22). The codes T1 through R4 denote the rubber type according to Table 1, while PE means the reference sample of plain HDPE.

The Young's modulus, *E*, decreases in the blends by 50%–60% while the yield stress, *Y*, also decreases, by 40%–50% as compared to plain HDPE. In the companion study [26] these changes have been compared with those predictable from theoretical models of Chow [28] and Nicholais and Narkis [29] developed for multi-component systems.

3.3. Toughness

Fig. 3 presents the notched Izod impact energies, I_s, of the rubber-modified HDPE measured at room temperature for the series of blends containing 0.22 vol. fraction of rubber. For each composition the results obtained for the specimens taken from the *gate end* and *far end* of the injection moulded bar are reported separately. The values of I_s obtained for *gate end* specimens show systematic deviation towards higher values which is caused by some flow-induced orientation present in the injection-moulded bar [26]. Fig. 3 demonstrates an impressive jump of the Izod impact energy, I_s, of HDPE when modified with rubbers. Moreover, the samples of plain HDPE broke nearly completely[2], while the behaviour of samples of rubber-modified HDPE was always of the '*non-break*' type[3]. Taking these observations into account, one can conclude that the relative toughness of rubber-modified HDPE to that of plain HDPE is even higher

[2] Partial or hinge breaks, according to classification suggested by ASTM D-256.

[3] At least 10% of the sample cross-section remained unbroken (ASTM D-256); in many of our blends up to 60%–70% of the sample cross-section remained unbroken.

than shown in Fig. 3. After the impact test a relatively large plastic deformation zone could be easily observed in the blend samples near the fracture flank. In this zone the material showed whitening. In addition, a reduction of the sample thickness close to the fracture flank was frequently observed. The whitened deformation zone in samples modified with rubber extended up to approximately 1 mm away from the fracture surface, whereas in unmodified HDPE no such deformation zone was observed.

The variation of impact energy within the group of blends with a 0.22 vol. fraction of rubber is very minor in comparison with the jump observed between plain HDPE and these blends. Nevertheless, within each class of the rubbers (i.e. amorphous EPDM, T1–T3; semi-crystalline EPDM, T4–T7; and EOR, R1–R4) one can notice a correlation between the rubber viscosity and the impact energy of the blend: I_s decreases with decreasing viscosity of the rubber component. On the other hand, the data presented in Table 3 suggest that the average size of rubber inclusions show similar correlation with rubber viscosity. Hence, one can expect that there exists a correlation between average rubber particle size and the toughness of the blend: for constant rubber concentration the Izod impact energy of the blends appears to increase with decreasing average particle size. In fact, such a correlation was frequently observed for other rubber-modified polymers [6,11,14,15].

The correlation of I_s and particle size can be observed even better in samples with rubber concentration lower than 0.22 reported above. Fig. 4 shows the plot of I_s against blend composition for HDPE modified with T1 and T7 EPDM rubbers (PE-T1 and PE-T7). The behaviour of HDPE modified with R1 and R4 EOR rubbers (PE-R1 and PE-R4) is very similar. In these figures, for every composition, but especially for those in the 0.1–0.2 vol. fractions range, I_s of the PE-T1 blend is higher than that of the PE-T7 blend, similarly I_s of the PE-R1 blend is higher than I_s of the PE-R4

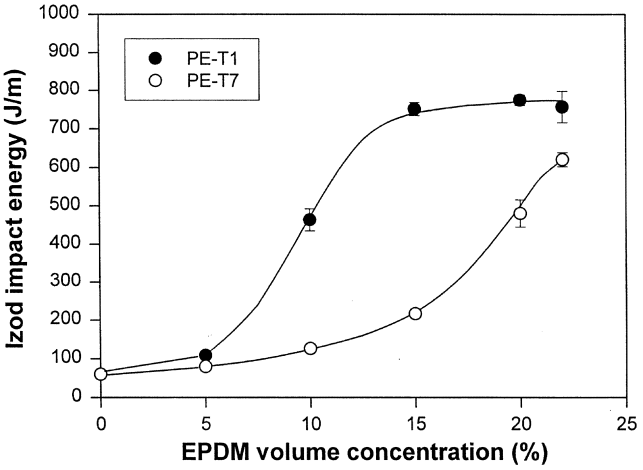

Fig. 4. The dependence of Izod impact energy on volume concentration of rubber in the HDPE modified with EPDM rubbers: (●) PE-T1 blends; (○) PE-T7 blends. Only the data for far end specimens are shown. The values obtained for gate end specimens were always slightly higher.

blend. Although we have estimated the average rubber particle sizes only in the samples containing 22% of these rubbers, these results can be extended over the whole composition range where the size of rubber inclusions is controlled primarily by the conditions of the mixing process (shear rate, temperature, time) and an interrelation of matrix and rubber properties at these processing conditions (e.g. dynamic viscosities). Since conditions of processing were identical for every sample produced, we expect that for a given type of rubber the size of its inclusions dispersed in the HDPE matrix should not depend on rubber concentration (in the range of interest), or at most this dependence should be very weak[4]. Thus, it seems justified to assume that the average size of rubber inclusions in the whole composition range is close to that determined for blends with 22% of rubber and reported in Table 3. Then, the data from Fig. 4 can be interpreted in the way that the impact energy of blends with smaller rubber particle size (PE-T1 and PE-R1) is larger than that of the blends with larger particles (PE-T7 and PE-R4, respectively) in a broad composition range. The shapes of the curves shown in Fig. 4 suggest, however, that although there is a correlation between rubber particle size and toughness of the system, particle size is not the main parameter which controls the toughness of the material. It may be anticipated that curves obtained for blends with larger rubber particles (i.e. PE-T7 and PE-R4) can be relatively easily transformed to coincide with those obtained for blends with smaller rubber particles (PE-T1 and PE-R1, respectively). As we discuss in Section 4.1 Wu [5] was first to propose and to demonstrate experimentally, for rubber-modified Nylon-6,6, that toughness of such systems depends neither on rubber inclusion size nor on rubber concentration alone, but correlates with the thickness of the matrix ligament between rubber particles.

Fig. 5 illustrates the dependence of toughness on test temperature of the HDPE–EPDM blends. The dependences in HDPE–EOR blends are very similar but show steep drops in toughness at somewhat higher temperatures. While HDPE exhibits nearly constant and very low impact energy over the whole temperature range studied (from −70°C to + 23°C), the blends show a pronounced ductile–brittle transition manifested in a jump of impact energy at a certain temperature, characteristic for a particular blend. Below this temperature the high toughness observed at higher temperatures precipitously diminishes to the level of HDPE. Clearly, the steep drop in toughness is a consequence of a glass transition in the rubber inclusions. We note that the increase of impact energy of the blends with decreasing temperature in the tough range is an artifact, and results from the fact that the blend samples become too compliant elastically and do not break completely in that temperature

[4] A possibility of noticeable coalescence of rubber inclusions during the mixing process of blends with higher rubber concentration, which would lead to an increase of average diameter of inclusions, is rather remote due to very high shear rate and relatively short time of mixing in the processing equipment employed in our study.

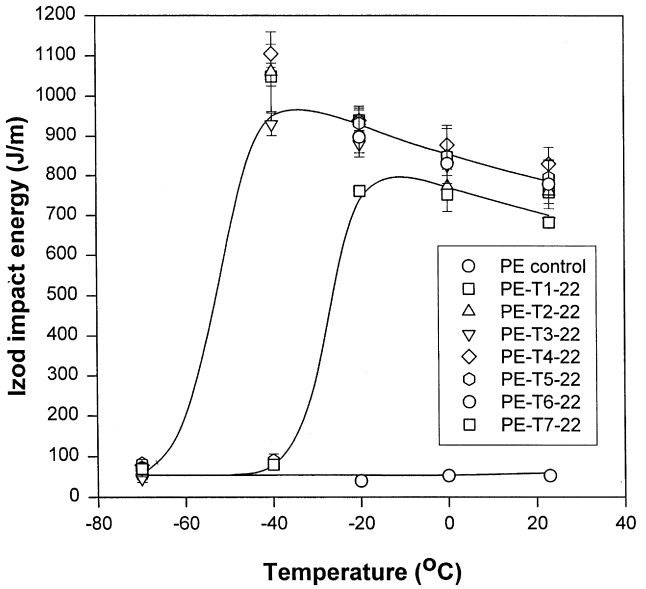

Fig. 5. The dependence of Izod impact energy on temperature in the HDPE modified with 0.22 vol. fraction of EPDM. Only the data for *far end* specimens are shown. The values obtained for *gate end* specimens were always slightly higher.

range. Then the partially cracked sample is elastically flexed through the machine. With decreasing temperature the length of the cracked region tends to increase and the energy becomes a better measure of the fracture process. To produce such an effect the toughness of the material had to actually decrease slowly with decreasing temperature.

Examination of fractured specimens demonstrated that, in the rubber-modified HDPE, tested at temperatures above the ductile–brittle transition temperature, extensive plastic deformation took place, manifested in a large whitened zone around the crack, whereas in the specimens tested below that temperature there was no trace of such plastic deformation zone and the morphology of the fracture surface revealed features similar to those observed in unmodified HDPE. This observation allows for a correlation of the ductile–brittle transition with properties of the rubbers. In the ductile region rubber is well above its glass transition temperature and, upon being stressed at the impact rates, the rubber inclusion cavitates readily with the onset of plastic response. This cavitation, in turn, allows unconstrained plastic deformation of the matrix ligaments, and results in the high impact energy absorption. However, when the temperature decreases, and the rubber undergoes a glass transition the well-adhered particles do not cavitate because of the greatly reduced mismatch of elastic properties with the matrix. This stifles the plastic deformation of the matrix and consequently results in brittle behaviour in impact. Thus, the temperature of the ductile–brittle transition can be directly related to the glass transition temperature of the rubber, which could be separately measured at frequencies corresponding to the deformation rate in the impact tests (i.e. at several tens of kHz). The EPDMs T1–T4 have their nominal glass transition temperature, T_g, in the range from -55 to -60°C (at low frequencies) and their blends show the ductile–brittle transition around -40°C while the blends with T5–T7 EPDMs having a nominal T_g around -45°C undergo a ductile–brittle transition near -20°C (cf. Fig. 5a). Similar relations can be observed for the HDPE–EOR blends, where R4 rubber has a higher T_g, consequently a higher ductile–brittle transition temperature than R1–R3 rubbers. While a counter argument could be advanced for this behaviour, based on considering the transition to brittle behaviour with decreasing temperature to be a direct demonstration of the role of the extensibility of the rubber in the toughening mechanism, that this is not so will become clearer in the companion study which follows, where, instead of rubber, $CaCO_3$ particles were used with substantially the same results [26].

The deformation induced during the Izod tests creates stress-whitened regions in the tough blends. As we already noted, the samples exhibiting super-tough behaviour did not break completely. The crack in these samples propagated with a substantial plastic process zone at its tip as the sample eventually bent sufficiently to allow the pendulum to swing by. In contrast, the brittle samples of plain HDPE or blends with low concentrations of rubber fractured nearly completely, and showed almost no stress-whitening around the fracture surface. To investigate the evolution of the deformation-induced morphology changes occurring in the super-tough blends during their high-speed deformation in the Izod impact experiment, samples were cryofractured in various directions after the test, as described in Section 2.3. The observations of morphology changes in the deformation zone were performed using the E-SEM. Since the morphology within the deformation zone in all super-tough blends look very similar, we limit the presentation here to representative micrographs of the blend PE-T1–22, tested at room temperature. On the other hand, the samples exhibiting brittle behaviour with no stress-whitening, gave nearly featureless SEM images. Therefore, the micrographs of such samples are not presented here.

Fig. 6 presents the IZOD1 view of the stress-whitened region of the PE-T1–22 sample. As seen in Fig. 1, the IZOD1 sampling plane is perpendicular to the fracture surface and parallel to the lateral surfaces of the specimen. The micrographs in Fig. 6a–d show the morphology containing cavities of the deformed blend at various depths with respect to the fracture surface. Far away from the fracture surface, near the end of the stress-whitened zone, the number density of cavities of nearly spherical shape is relatively low, indicating that only a fraction of rubber particles have cavitated (see Fig. 6a). Fig. 6b–d demonstrates that the number density of cavities increases when moving through the stress-whitened zone towards the fracture surface. Eventually, in the region just beneath the fracture surface, the number density of cavities is so large that nearly all rubber particles present in this region appear to have cavitated (Fig. 6c,d). Simultaneously, the shape of the cavities also change pro-

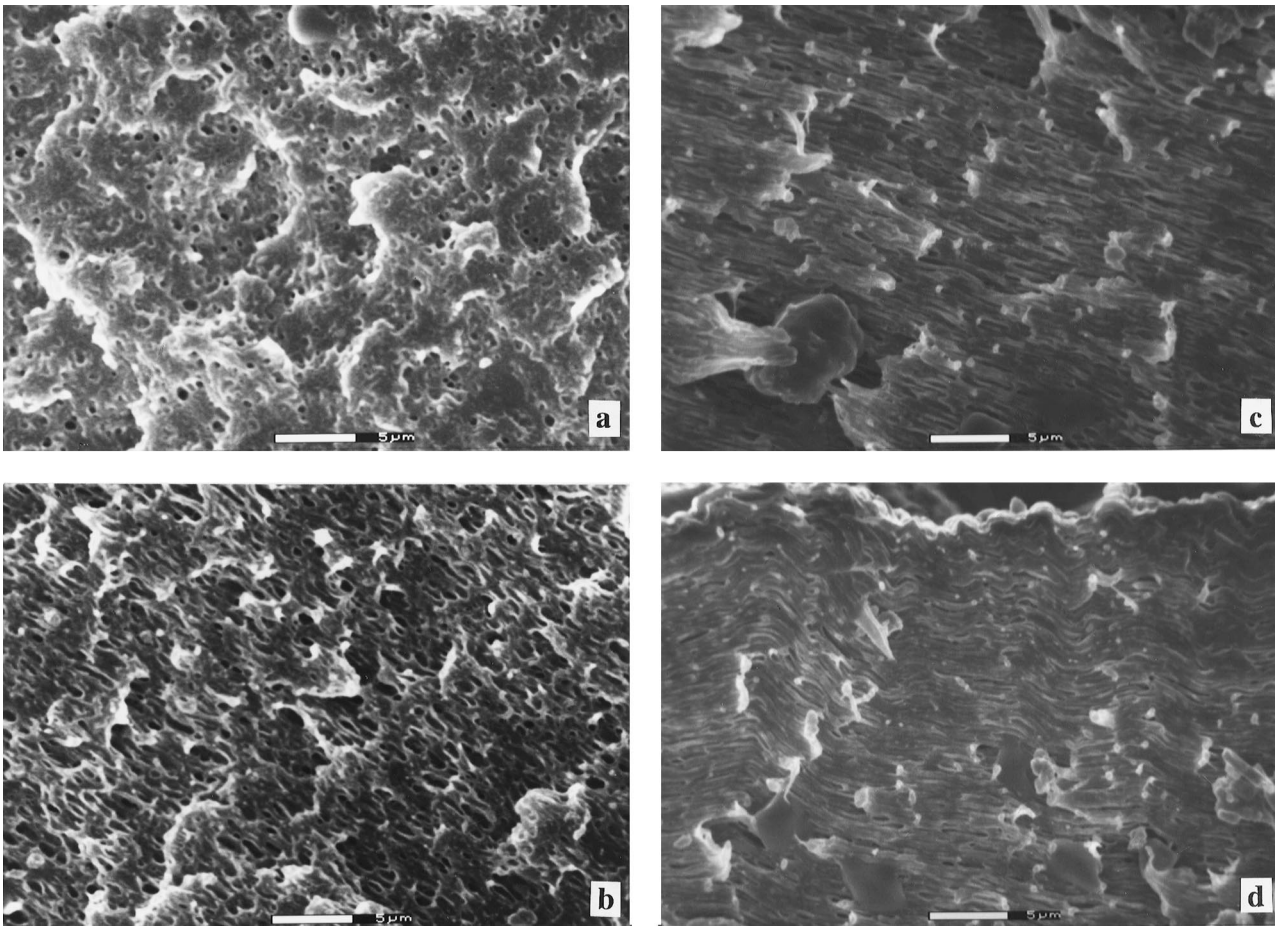

Fig. 6. IZOD1 sampling view of sample PE-T1–22 taken inside the stress-whitened zone at various distances away from the fracture surface: (a) 600, (b) 200, (c) 50 and (d) 0 μm from the fracture surface, respectively.

gressively: from spherical, at the end of the whitened zone, to highly elongated shapes close to the fracture surface, where the cavities reach lengths of up to several micrometres. Observation of cavities in the IZOD2 view, perpendicular to IZOD1, reveals that the cavities have usually circular cross-sections. Fig. 7 shows the same PE-T1–22 sample in the IZOD2 view at a depth from the fracture surface corresponding to that shown in Fig. 6c. Closer examination of the shape of cavities in the IZOD1 and IZOD2 views leads to the conclusion that the elongated cavities are of nearly cylindrical shape (more appropriately, sausage shape) with diameters nearly constant along their entire length. Another observation is that the diameter of both spherical (at the end of the stress-whitened zone) and cylindrical (closer to the fracture surface) cavities is fairly constant and very close to the diameter of the rubber inclusions, which were 0.5 μm in this blend. The only exceptions were the cavities located right below the fracture surface, which were narrower (cf. Fig. 6d), and were additionally frequently bent or buckled. The specific shape and smaller thickness of these cavities near the fracture surface will be discussed below.

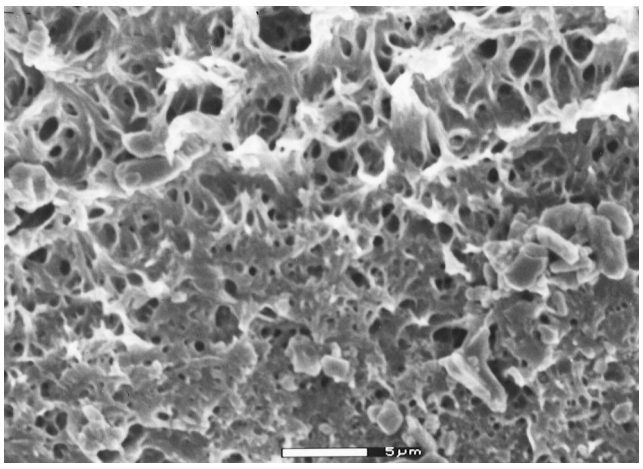

Fig. 7. IZOD2 sampling view of sample PE-T1–22 taken inside the stress-whitened zone close to the fracture surface.

The length (or aspect ratio) of the cylindrical cavities is a measure of the extent of plastic strain undergone by the matrix ligaments while their orientations change gradually from roughly perpendicular to the fracture surface at depth to nearly parallel to the fracture surface in the region just below it, graphically demonstrating the changing principal stretch direction in various locations below the fracture plane [12]. This indicates that the plastic strain experienced

by the matrix ligaments between cavities increases markedly when approaching the fracture surface, where it reaches values close to the ultimate elongation of polyethylene. This clearly demonstrates massive plastic deformation of the matrix ligaments which is the main source of the high toughness of the blends and is a consequence of almost entirely of crystallographic deformation processes (see Section 4). The changing aspect ratio of cavities in the stress-whitened zone represents the local residual stretch, that changes from approximately 10 to 1 within the deformation zone, of ca. 1 mm thickness, from the fracture surface into the interior. However, most of this change is limited to approximately the first 50 μm from the fracture surface, where changes in the cavity orientation are also the strongest. Therefore, this relatively thin surface layer is the zone of very intense plastic deformation left by the crack. It occupies only ca. 5% of the volume of stress-whitened zone but accounts for much more than 50% of the total strain produced in that zone. The local residual stretch of the order of 10, parallel to the fracture surface, can be observed in a thin layer immediately beneath the crack flanks (cf. Fig. 6d).

The characteristic sausage-like shape of the cavities and their almost constant diameter for the whole range of strain suggest that the matrix ligaments deformed plastically by extensive shear, localized mostly in the regions between the poles and the equator of the rubber particles (in relation to the axis of principal stretch of the local region). At the same time the PE matrix near the polar regions of the rubber particles remained practically undeformed. These features that are very similar to those reported by Muratoglu et al. [12,13] in Nylon are supported also by computer simulations of Tzika et al. [32], of the stretch of a representative cavity, surrounded by material with the representative plastic anisotropy.

Fig. 8 shows the view of the fracture surface of the same PE-T1–22 blend. This surface is dominated by regularly spaced striations oriented perpendicular to the direction of crack propagation (from right to left on the micrograph). The features observed on this micrograph are typical for all blends studied in their tough region, regardless of the type of particular rubber or its concentration. In contrast, in the brittle regime, i.e. in plain HDPE and the blends with the lowest rubber content or those tested at low temperatures, the fracture surface is macroscopically rather smooth with only irregular features, resembling those typical for brittle failure [3]. Similar morphology of the fracture surface filled with striations was observed by several authors in rubber-modified Nylon 6 and 6,6 [4,31,32], and was explained in detail by Muratoglu et al. [13]. Consistent with the earlier work [13], Fig. 6d clearly shows that in the near-surface layer of approximately 30 μm thickness, the material undergoes periodic buckling and folding, accompanied by partial healing of the cavities, which are noticeably thinner in this layer than in the material located at intermediate depths (compare Fig. 6c,d). The folds within this highly stretched layer, visualized by the folded cavities, match exactly the folds observable on the cross-section of the fracture flank (seen in upper part of Fig. 6d) and, of course, the striations observable on fracture surface of Fig. 8.

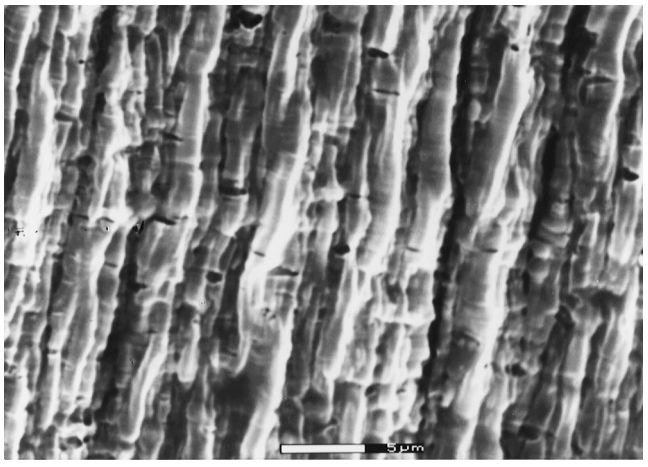

Fig. 8. Fracture surface of PE-T1–22 sample. The direction of crack propagation is from right to left.

4. Discussion

4.1. The critical matrix ligament thickness criterion

In his pioneering study of Nylon-6,6/rubber blends Wu [4,5] found that a sharp brittle–tough transition occurs when the average thickness Λ of the matrix ligaments between rubber particles is smaller than a certain critical value, Λ_c. This critical value is independent of rubber volume fraction and particle size, and is the property of the matrix alone. He proposed that this distance is the key parameter determining whether a blend will be brittle or tough.

For a blend with dispersed spherical particles of equal diameter, d, the thickness Λ of the matrix ligaments can be expressed by the equation [5]:

$$\Lambda = d[\beta(\pi/6\varphi)^{1/3} - 1] \quad (1)$$

where φ is volume fraction of these particles and β is a geometric constant, depending on the packing of the particles (1.0 for simple cubic packing; $(3)^{1/2}(2)^{2/3} = 1.09$ for body-centred cubic; and $(2)^{1/6} = 1.12$ for face-centred cubic packing[5]). For the blends of Nylon 6,6 with rubber Wu chose a simple cubic packing as a preferred approximation for the real spatial arrangement of the rubber particles in the Nylon matrix.

Eq. (1) was derived under the assumption of equal size particles and regular packing. However, in real blends the particle sizes frequently obey a log-normal distribution [33],

[5] The vaues of β for BCC and FCC packing differ from those reported by Wu ($2^{1/3}$ and $4^{1/3}$, respectively[5]) suggesting a geometrical misinterpretation in his estimates.

characterized by two parameters: the geometrical mean size $\langle d_{gn} \rangle$ (equal to the median size by count) and the geometrical mean standard deviation, σ, being the measure of polydispersity ($\sigma = 1$ for monodisperse distribution, and $\sigma > 1$ for polydisperse distributions). The mean ligament thickness for the blend with particles with a size distribution characterized by a geometrical standard deviation σ can be described by [5]:

$$\Lambda(\sigma) = \Lambda_o \exp[(\ln \sigma)^2] \quad (2)$$

hence:

$$\Lambda(\sigma) = d[\beta(\pi/6\phi)^{1/3} - 1] \exp[(\ln \sigma)^2] \quad (3)$$

where $\Lambda_o = \Lambda(\sigma = 1)$. The above equations should be additionally modified by a term describing dispersion of rubber particles in the HDPE matrix. If the dispersion is not perfect and flocculation or aggregation occurs, the average ligament thickness increases. However, since experimental data were insufficient to implement such modification, a perfect dispersion of the rubber particles was assumed which, of course, results in some underestimation of the critical length Λ_c.

To examine the dependence of impact energy on matrix ligament thickness in the blends investigated in this study, Eq. (3) was used together with parameters of the rubber particle size distributions given in Table 3 to calculate a ligament dimension for the blends PE-T1, PE-T7, PE-R1 and PE-R4. For these calculations it was assumed that the particle size distribution for a given blend (rubber type) does not change with the rubber content in the volume concentration range of 0.05–0.22, as discussed in the previous section. The results of the calculations are presented in Fig. 9, which demonstrates that the data of Izod impact energy, obtained for the blends of HDPE with four various rubbers in a broad range of compositions follow a single curve when plotted as a function of average matrix ligament thickness. This clearly demonstrates that the criterion of toughening given by Wu has merit and can be applied also to the HDPE-based blends of the present study. The 'master curve' presented in Fig. 9 exhibits the jump of impact strength when the average ligament thickness decreases below $\Lambda = 0.6$ μm. This value can then be considered as the critical thickness, Λ_c for the specific HDPE matrix used here. It is different (higher) than the values determined previously for Nylon 6,6 ($\Lambda_c = 0.3$ μm [5]) or isotactic polypropylene ($\Lambda_c = 0.15$ μm [17]). This comparison indicates clearly that the Λ_c parameter is indeed matrix-specific, i.e. it depends on the nature and properties of the matrix and not on the nature of the rubber particles dispersed in that matrix.

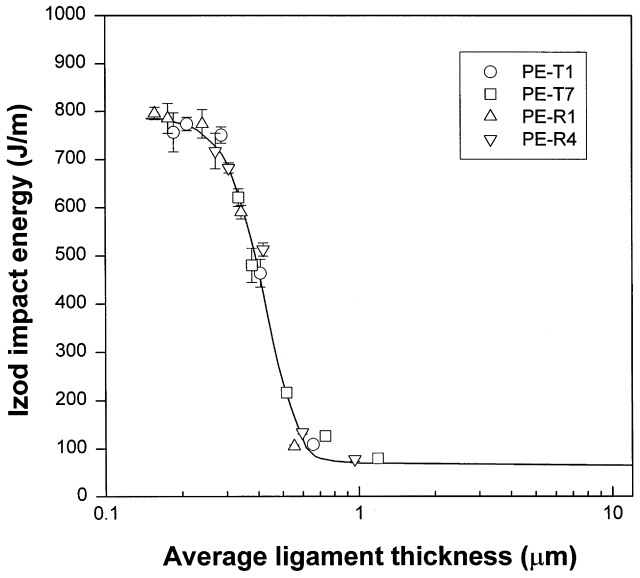

Fig. 9. The 'master plot' of Izod impact energy versus matrix ligament thickness obtained for PE-T1, PE-T7, PE-R1 and PE-R4 using the data taken from Fig. 4 and EOR rubbers.

We note here a difference of the plots in impact energy as a function of matrix ligament thickness presented by Wu [5] and that reported in this study. In the plot of Wu [5] for Nylon-based blends in the range of $\Lambda < \Lambda_c$ the curve splits into separate branches where the level of impact energy depends on the actual composition of the blend. In the plot for the rubber-modified HDPE presented in Fig. 9, all data points follow the same master curve for the entire composition range and do not indicate any tendency to split in the high toughness (small ligament thickness) range. At present we have no definitive explanation for this difference and conclude that more experimental data in the range of tough behaviour ($\Lambda < \Lambda_c$) is needed for HDPE to resolve this issue.

4.2. Relation of Λ_c to morphology and mechanism of plastic deformation

The transition from brittle to tough response of the rubber-toughened Nylon 6,6 blends, occurring at a critical ligament thickness Λ_c, was explained by Muratoglu et al. [12] by the mechanism depicted in Fig. 10a,b. On the basis of detailed morphological studies based on TEM, SEM and wide-angle X-ray scattering [15], they found that crystallization of Nylon from the melt is initiated from the incoherent Nylon–rubber interface and leads to the formation of crystallographically oriented material in the near-interface layer of Nylon, of approximately 0.15 μm thickness, in which the Nylon crystallites grow in a preferential manner with their (001) crystallographic planes parallel to the interface. The (001) plane in monoclinic Nylon 6 and Nylon 6,6 is known to be a low energy plane containing hydrogen bonds [34], and also has the lowest crystallographic slip resistance [16]. If the thickness of this oriented crystallization layer between particles is less than 0.3 μm, a high concentration of the material with reduced anisotropic plastic resistance is placed at the borders of particles where it promotes ready stretch of ligaments and plastic response of the entire assembly through the percolation of this material throughout the structure as depicted in Fig. 10b. If,

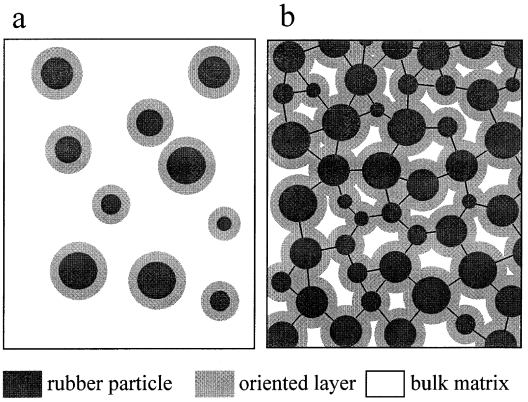

Fig. 10. Schematic representation of the layer of crystallites of preferred orientations: (a) when ligament thickness is larger than twice the thickness of the oriented crystallization layer and material exhibits brittle behaviour; (b) when ligament thickness is less than twice the thickness of the oriented crystallization layer around the particles and material with reduced plastic resistance percolates through the blend. The light grey represents the oriented layer of the matrix, while the connecting lines show the orientation of lamellae in interparticle ligaments(drawn after Ref. [12]).

however, the oriented layers of reduced plastic resistance around particles do not percolate through the structure, when $\Lambda > \Lambda_c$ ($\Lambda > 0.3\ \mu$m) as depicted in Fig. 10a, the overall matrix plastic resistance is substantially elevated due to a higher concentration of randomly oriented crystallites filling-in in the background. Then, premature fracture occurs governed by the extrinsic flaws responsible for brittle behaviour. As already stated, the morphological and microstructural features of this mechanism were extensively documented by TEM, SEM and WAXS and various free-standing thin film experiments to put it on a definitive foundation in Nylon [15].

The same model applies also to the blends of HDPE with rubbers reported here. In support of this proposition the crystallization habits and orientation of polyethylene crystallites were studied in detail in thin films. These films, with a range of thicknesses, were crystallized from the melt in contact with layers of rubber on both sides of the films [35]. For this the same HDPE and one of the rubbers used in the present study (R3EOR rubber) were used and the morphology was monitored both by WAXS and atomic force microscopy. It was found that the incoherent HDPE–rubber interface induces a strong specific crystallization habit of HDPE in the near-interface layers, of up to 0.4 μm thickness. Lamellar HDPE crystallites were found oriented preferentially edge-on, with their lamellar normals parallel or slightly tilted with respect to the interface plane. The crystallographic (100) planes of these crystallites were found oriented preferentially parallel to the interface plane giving a direct correspondence to the morphology established by Muratoglu et al. [12] in their Nylon 6 thin films. Because of a direct correspondence of all features of crystallization between HDPE and Nylon, additional TEM studies of rubber modified HDPE were considered unnecessary. These crystallization studies are described in detail in the third companion study (III) [35], together with corresponding measurements made for crystallization against calcite single-crystal surfaces, in support of the immediately following accompanying study (II) [26].

From the point of view of mechanical properties of the HDPE/rubber blends the anisotropy of the above-mentioned oriented near-interface crystallization layers is extremely important. As is well established, PE crystallites deform plastically by crystallographic slip, twinning and martensitic transformations [18,36]. Moreover, for strains in excess of 0.1–0.15, where the amorphous component 'locks-up' and ceases to deform further, all large strains are derived almost entirely from crystallographic slip processes [19,37–41]. Two of these crystallographic mechanisms, the chain slip system (100)[001] and the transverse slip system (100)[010] operate in the (100) plane in the direction of the chain and transverse to it, respectively. It was found [19] that these slips have the lowest plastic resistances among all other deformation mechanisms active in polyethylene crystals. The plastic resistances were found to be 7.2 MPa for the (100)[001] chain slip system and 12.2 MPa for the (100)[010] transverse slip system, respectively, while the resistance of the third principal slip systems, (010)[001] chain slip, was 15.6 MPa [19]. This indicates that the plastic shear by chain slip in the (100) plane is much easier to activate than any other deformation mechanism in polyethylene crystals. In the case of random orientation of chains in the (100) planes parallel to the interface, the average resistance for shear in this collection of planes can be estimated to be below 10 MPa. Thus, there is a complete analogy in HDPE to the crystallization habits and their mechanical consequences observed in Nylon 6 crystallized in thin films, in which the crystallographic (001) plane, with its lowest energy and lowest plastic resistance, orients preferentially parallel to the interface with a rubber substrate [15].

The specific crystallization habits and resulting orientations observed in the thin films of HDPE, as reported above, should be present around the spherical rubber particles since the radii of curvature of these particles are large in comparison with the scale of the primary and secondary nuclei, of the crystallites forming adjacent to the particle/matrix interface. These nuclei are expected to be in the nanometre range. Therefore, it can be expected that substantially the same type of crystallite orientation will develop in both the near-interface layers in thin films deposited on flat substrates and the thin layers around rubber inclusions in the blends. The TEM observations of Muratoglu et al. [12], and the results of corresponding studies in the HDPE/rubber system [35], furnish very strong support for this morphology. Thus, the morphology of the HDPE/rubber blends shows a striking similarity to that found in Nylon 6,6/rubber blends, with rubber inclusions being surrounded by shells of oriented polyethylene crystallites in which the (100) crystallographic planes of lamellar crystallites become parallel to the interface and lamella normals are oriented tangentially

with respect to the particle periphery; the overall microstructure is shown schematically in Fig. 10. The thickness of the oriented shell of HDPE encapsulating every rubber inclusion is expected to be 0.2–0.4 μm and independent of the diameter of the rubber inclusion. When the mean ligament thickness is below 0.6 μm the oriented anisotropic material of reduced plastic resistance should percolate through the structure. The thickness of the near-interface oriented crystalline layers is larger for HDPE than that found for Nylon 6,6, where it was around 0.15 μm [15], but otherwise the morphology of the HDPE and Nylon 6-based blends show nearly identical features.

Considering all of the above facts we postulate that the mechanism of the toughening of HDPE with rubbers is the same as that proposed for Nylon 6,6 [12] and discussed earlier in this section. The only difference is the thickness of the shell formed by oriented crystallites around rubber inclusions. Such difference is expected for various polymers because of differences in their crystal structure as well as different energetic and kinetic parameters of their crystallization. Consequently, the critical ligament thickness at which oriented layers around adjacent inclusions merge and at which the toughness jump can be observed, is estimated as $\Lambda_c \approx 0.3$ μm for Nylon 6,6 [4,12] and $\Lambda_c \approx 0.6$ μm for HDPE.

According to the postulated mechanism, the plastic deformation upon impact of the blends, in their tough region ($\Lambda < \Lambda_c$), begins by cavitation of the rubbery particles due to deformation-induced negative pressures built up in them resulting from their very different elastic properties in the range where the rubbers are above their T_g. This, in turn, transforms the deforming blend into a randomly arranged cellular material in which the interparticle ligaments become cell walls and are composed of preferentially oriented lamellar crystallites with the best slip planes being oriented parallel to the interfaces, which now become the free surfaces of the cavities. Under these conditions the sectors of the cavities making approximately 45° angles with the major principal local stretch direction will readily undergo deformation by chain slip and transverse slip in the (100) planes (accompanied by the required deformation of the intervening amorphous component). At the same time the sectors of the cavity surface perpendicular to the local stretch direction should deform little since there is no resolved shear stress in these regions. This should then result in the stretching out of the matrix ligaments between cavities to produce the sausage-shaped cavities, as depicted in Fig. 11 [12]. However, some morphological evidence suggests that the equatorial regions around cavities also undergo extensive plastic stretching perhaps by the development of complex constraints between these regions and the deforming sectors. The mechanisms of this deformation need further study. Such postulated shapes of the cavities was confirmed by both experimental observations (reported in Section 3 and in Ref. [12]) as well as being verified in ongoing computer simulations of rubber cavitation and cavity evolution in the oriented matrix material [32]. Eventually, the stretched ligaments reach the ultimate draw ratio, characteristic of the HDPE matrix, and fail, leading to the development of a crack. In contrast, in the brittle samples, with ligament thicknesses well above 0.6 μm, the overall deformation resistance remains high because the matrix is dominated by its topologically continuous, randomly oriented fraction of crystallites of higher plastic resistance and fracture is precipitated prematurely from a notch, a non-characteristically large impurity particle or a structural flaw, before much overall plastic stretch takes place.

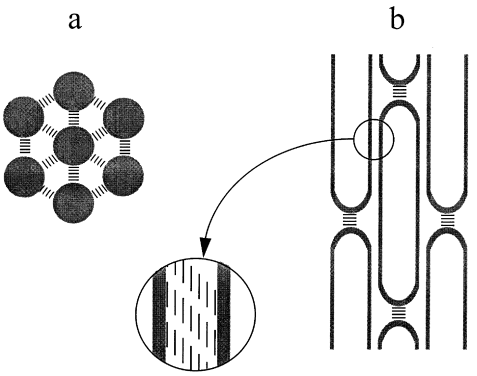

Fig. 11. Schematic diagram for the deformation mechanism of an idealized morphology under tensile deformation: (a) before and (b) after deformation. The parallel lines between particles and cavities represent the traces of (100) planes of HDPE (or (001) planes of Nylon) oriented crystallites. The grey shades represent the rubber (drawn after Ref. [12])

It is important to point out that the special toughening mechanism remains operating at the required high impact deformation rates because of the relatively lower rate sensitivity of the crystallographic mechanism of deformation and establishes a very reliable amelioration of the notch brittleness of the HDPE. This is a further demonstration that the much more rate-dependent deformation of the amorphous component of the HDPE does not govern the response.

5. Conclusions

The results reported here demonstrate that rubber-toughened polyethylene undergoes a brittle-to-tough transition when the thickness of the matrix ligaments between adjacent rubber particles become less than a critical dimension. This critical thickness does not depend on the type of rubber or its concentration, or the size of the rubber particles, and it is exclusively the property of the polymer matrix alone. The impact energies of blends of HDPE with various rubber particles of a variety of sizes incorporated into the blend at various volume fractions exhibit a single behaviour pattern when plotted against matrix ligament thickness. Such toughness transitions of rubber-modified polyethylene are identical in form to that observed in Nylon 6,6 or isotactic polypropylene modified with EPDM rubbers [5,11,12,17].

The critical matrix ligament thickness, Λ_c, found for HDPE is approximately 0.6 μm.

The high levels of toughness of these materials is a result of the specific oriented crystallization found in the matrix layers of certain thickness around each rubber inclusion. In these layers, polyethylene crystals are oriented with their low-energy easy-to-shear (100) planes parallel to the HDPE/rubber interfaces. When the ligament thickness decreases below the critical value, characteristic for a given matrix, the oriented layers around adjacent rubber particles merge into a percolating material component of reduced plastic resistance. This results in substantial reduction of overall plastic resistance of the material, prevents initiation of fracture from the unavoidable strength-controlling imperfections and effectively eliminates the notch brittleness of the material, resulting in dramatic toughening.

The crystal structure and crystallization habits of polyethylene and Nylon are substantially different. Nevertheless, the same mechanisms utilizing interfacial interactions between components of the blend prior to matrix crystallization were found responsible for formation of the same special type of well-organized crystalline lamellae morphology in both polymers modified with rubber. This suggests that the mechanism of toughening proposed initially to explain only the behaviour of rubber-modified Nylon 6,6 [12] is general and controls the toughening of semi-crystalline polymers with potentially widespread application. That this is indeed the case is demonstrated further in the accompanying study utilizing calcium carbonate fillers in the place of rubbers where nearly identical end results were achieved [26].

The postulated model of toughening leads to another important conclusion. It is a widely held opinion in the practice of rubber toughening of polymers that grafting of the rubber particle to the matrix is essential for achieving strong adhesion to result in effective stress transmission, and subsequent cavitation of the rubber upon deformation. The latter is based on the premise that the high toughness of the rubber-modified material is derived from cavitation itself. In the light of the proposed mechanism this point of view is found to be unfounded. In the present study, grafting of rubber to the matrix was important and even essential to obtain a tough material where, however, its primary role was to produce better dispersion of the rubber component in the matrix to achieve a tighter ligament thickness distribution, rather than directly increase toughness by any substantial amount. For many polymer pairs the dispersion obtained by simple blending of components, without application of grafting, results in wide distributions of particle sizes and interparticle ligament thicknesses, which adversely affects the all-important percolation condition of material of reduced plastic resistance. While cavitation itself is known to result in some toughening by crack-tip shielding, this effect is relatively minor [42]. In the context of the toughening mechanism discussed in this study the state of adhesion of the rubber particle is of little importance provided the particle results in preferential crystallization and cavitates to permit the matrix with enhanced plastic compliance to deform freely. If debonding of particles is an option in place of cavitation; the rubber particles could be replaced with rigid filler particles to also improve the modulus of the blend. This possibility is discussed in detail in the accompanying communication [26].

Acknowledgements

This research was supported primarily by the MRSEC Program of the National Science Foundation under award number DMR 94-00334 and has also made use of the Shared Facilities of the CMSE at M.I.T. supported under the same program. The exploratory blends were produced in the facilities of the DuPont Company under the direction of MW.

References

[1] Arends CB, editor. Polymer toughening. New York: Marcel Dekker, 1996.
[2] Martuscelli E, Musto P, Ragosta G, editors. Advanced routes for polymer toughening. Amsterdam: Elsevier, 1996.
[3] Ward IM. Mechanical properties of solid polymers, 2nd ed. New York: Wiley, 1983.
[4] Wu S. Polymer 1985;26:1855.
[5] Wu S. J Appl Polym Sci 1988;35:549.
[6] Margolina A, Wu S. Polymer 1988;29:2170.
[7] Borggreve RJM, Gaymans RJ. Polymer 1989;30:63.
[8] Oshinski AJ, Keskkula H, Paul DR. Polymer 1992;33:267.
[9] Majumdar B, Keskkula H, Paul DR. Polymer 1994;35:1399.
[10] Dijkstra K, ter Laak J, Gaymans RJ. Polymer 1994;35:332.
[11] Borggreve RJM, Gaymans RJ, Schuijer J, Ingen Housz JF. Polymer 1987;28:1489.
[12] Muratoglu OK, Argon AS, Cohen RE, Weinberg M. Polymer 1995;36:921.
[13] Muratoglu OK, Argon AS, Cohen RE, Weinberg M. Polymer 1995;36:4771.
[14] Karger-Kocsis J, editor. Polypropylene: structure, blends and composites. London: Chapmann & Hall, 1995.
[15] Muratoglu OK, Argon AS, Cohen RE, Weinberg M. Polymer 1995;36:2143.
[16] Lin L, Argon AS. Macromolecules 1992;25:4011.
[17] Wu X, Zhu X, Qi Z. In: The 8th International conference on deformation, yield and fracture of polymers. London: The Plastics and Rubber Institute, 1991:78/1.
[18] Bowden PB, Young RJ. J Mater Sci 1974;9:2034.
[19] Bartczak Z, Argon AS, Cohen RE. Macromolecules 1992;25:5036.
[20] Knight GW. In: Arends CB, editor. Polymer Toughening, ch. 7. New York: Marcel Dekker, 1996:189.
[21] Kapuscinski M, Schreiber HP. Polym Eng Sci 1979;19:900.
[22] Kalfaoglu NK. J Macromol Sci Phys 1983;22:343; Kalfaoglu NK. J Macromol Sci Phys 1983;22:363.
[23] Fortelny I, Kovar J, Sikora A, Hlavata D, Krulis Z, Novakova Z, Pelzbauer Z, Cefelin P. Angew. Makromol Chem 1985;132:111.
[24] D'Orazio L, Greco R, Mancarella C, Martuscelli E, Ragosta R, Silvestre C. In: Galeski A, Kryszewski M, Martuscelli E, editors. Polymer blends: processing, morphology, properties, vol 2. New York: Plenum Press, 1984:111.

[25] Greco R, Mancarella C, Martuscelli E, Ragosta G, Jinghua Y. Polymer 1987;28:1922.
[26] Bartczak Z, Argon AS, Cohen RE, Weinberg M. Polymer 1999;40:2347.
[27] Wunderlich B, Cormier CM. J Polym Sci Part A-2 1967;5:987.
[28] Chow TS. J Polym Sci Polym Phys Ed 1978;16:959.
[29] Nicolais L, Narkis M. Polym Eng Sci 1971;11:194.
[30] Flexman EA. Polym Eng Sci 1979;19:564.
[31] Speroni F, Castoldi E, Fabricci C, Casiraghi F. J Mater Sci 1989;24:2165.
[32] Tzika P, Boyce MC, Parks DM. (to be published).
[33] Irani RR, Callis CF. In: Particle size: measurement, interpretation and application. New York: Wiley, 1963.
[34] Galeski A, Argon AS, Cohen RE. Makromol Chem 1987;188:1195.
[35] Bartczak Z, Argon AS, Cohen RE, Kowalewski T. Polymer 1999;40:2367.
[36] Lin L, Argon AS. J Mater Sci 1994;29:294.
[37] Galeski A, Bartczak Z, Argon AS, Cohen RE. Macromolecules 1992;25:5705.
[38] Bartczak Z, Cohen RE, Argon AS. Macromolecules 1992;25:4692.
[39] Bartczak Z, Argon AS, Cohen RE. Polymer 1994;35:3427.
[40] Lee BJ, Parks DM, Ahzi S. J Mech Phys Solids 1993;41:1651.
[41] Lee BJ, Argon AS, Parks DM, Ahzi S, Bartczak Z. Polymer 1993;34:3555.
[42] Argon AS, Cohen RE, Muratoglu OK. In: Boyce MC, editor. Mechanics of Plastics and Plastic Composites. New York: ASME. 1995;MD vol. 68/AMD vol 215:177.